Bi-substituted Effect on Phenylisoquinoline Iridium(III) Complexes

Yu-Ting Huang, Ta-Hsien Chuang, Yu-Lin Shu, Yi-Chun Kuo, Pei-Lin Wu,* Cheng-Hsien Yang,* and I-Wen Sun*

Department of Chemistry, National Cheng Kung University, Tainan, Taiwan, 70101, Republic of China

Received July 27, 2005

This paper studies the synthesis and photophysical properties of a series of bi-substituted phenylisoquinoline iridium(III) complexes. Interestingly, the bis[3-methyl-1-*p*-tolylisoquinolinato-*N*,$C^{2'}$] iridium(III) (acetylacetonate) (**6a1**) could be prepared even though the single-crystal X-ray crystallography data showed that there was steric hindrance due to the methyl group on the C-3 position to isoquinoline. Noticeably, the cyclic voltammetric (CV) measurements indicated that although these iridium(III) complexes have similar energy gaps, their $E_{1/2(ox)}$ are different from the mono-substituted (in phenyl ring) phenylisoquinoline iridium(III) complexes. This illustrates that the major influence of oxidation potential for iridium(III) complexes is the substituted isoquinoline ring. While all these complexes emitted in the red region, the bis[5-methyl-1-*p*-tolylisoquinolinato-*N*,$C^{2'}$] iridium(III) (acetylacetonate) (**6c1**) showed a higher brightness of 9299.36 cd/m^2 at a higher current density of $J = 63.69$ mA/cm^2 and a better luminance efficiency of 21.96 cd/A at a current density of $J = 0.28$ mA/cm^2. The corresponding CIE (Commission International de L'Eclairage) coordinates are $x = 0.67$, $y = 0.33$.

1. Introduction

As a promising technology for flat panel displays, organic light-emitting diodes (OLEDs) have attracted a great deal of attention since 1987.[1−3] In recent years, phosphorescent dyes were doped into charge-transporting hosts as emissive layers because of their high emission efficiency compared to the conventional fluorescent OLEDs.[4−6] These dyes include the square planar d^8 complexes of Pt(II),[7] Pd(II),[8] and Au(III)[9] and octahedral d^6 complexes of Ru(II),[10] Rh(III),[11] Ir(III),[12] and Pt(IV).[13,14] The strong spin−orbit coupling, caused by the heavy metal atom, makes the intersystem cross from the singlet to the triplet excited states more efficiently. In theory, the mixing of the singlet and triplet excited states can lead to an internal phosphorescence quantum efficiency for the OLEDs of as high as ∼100%. Because of this fact, more and more research focuses on the phosphorescent materials for the application of OLEDs.

Ir(piq)$_3$ [iridium(III) tris(1-phenylisoquinolinato-*N*,$C^{2'}$)] is a famous red phosphorescent emitter, which exhibits a maximum saturated red emission peak at 623 nm, and the efficiency of the electroluminescence device is 8.0 lm/W, 9.3 cd/A at 100 cd/m^2.[15] More extended works have been published by Su,[16] Yang,[17] and Rayabarapu.[18] However, none of these have focused on discussing the bi-substituted ligand effect on the iridium(III) complex. In this paper, we report a series of high-efficiency red phosphorescent iridium(III) complexes based on the bi-substituted ligand.

2. Experimental Section

General Information and Materials. Scheme 1 outlines how the phenylisoquinoline ligands were synthesized and

* Corresponding author. Tel: +886-6-2757575-65355. Fax: +886-6-2740552. E-mail: iwsun@mail.ncku.edu.tw.

(1) Tang, C. W.; Vanslyke, S. A. *Appl. Phys. Lett*. **1987**, *51*, 913.
(2) Fukuda, Y.; Wakimoto, T.; Miyaguchi, S.; Tsuchida, M. *Synth. Met.* **2000**, *111−112*, 1.
(3) Kubota, H.; Miyaguchi, S.; Ishizuka, S.; Wakimoto, T.; Funaki, J.; Fukuda, Y.; Watanabe, T.; Ochi, H.; Sakamoto, T.; Miyake, T.; Tsuchida, M.; Ohshita, I.; Tohma, T. *J. Lumin.* **2000**, *87−89*, 56.
(4) Tang, C. W.; VanSlyke, S. A.; Chen, C. H. *J. Appl. Phys*. **1989**, *65(9)*, 3610.
(5) Wang, X.; Rundle, P.; Bale, M.; Mosley, A. *Synth. Met.* **2003**, *137*, 1051.
(6) Tokito, S.; Tsuzuki, T.; Sato, F.; Iijima, T. *Curr. Appl. Phys*. 2005, *5*, 331.
(7) (a) Chassot, L.; von Zelewsky, A. *Inorg. Chem.* **1987**, *26*, 2814. (b) Sandrini, D.; Maestri, M.; Balzani, V.; Chassot, L.; von Zelewsky, A. *J. Am. Chem. Soc.* **1987**, *109*, 7720.
(8) Gianini, M.; Forster, A.; Haag, P.; von Zelewsky, A.; Stoeckli-Evans, H. *Inorg. Chem.* **1996**, *35*, 4889.
(9) Parish, R. V.; Wright, J. P.; Pritchard, R. G. *J. Organomet. Chem.* **2000**, *596*, 165.
(10) (a) Reveco, P.; Schmehl, R. H.; Cherry, W. R.; Fronczek, F. R.; Selbin, J. *Inorg. Chem.* **1985**, *24*, 4078. (b) Reveco, P.; Medley, J. H.; Garber, A. R.; Bhacca, N. S.; Selbin, J. *Inorg. Chem.* **1985**, *24*, 1096.
(11) (a) Sprouse, S.; King, K. A.; Spellane, P. J.; Watts, R. J. *J. Am. Chem. Soc.* **1984**, *106*, 6647. (b) Ohsawa, Y.; Sprouse, S.; King, K. A.; DeArmond, M. K.; Hanck, K. W.; Watts, R. J. *J. Phys. Chem.* **1987**, *91*, 1047.
(12) (a) King, K. A.; Spellane, P. J.; Watts, R. J. *J. Am. Chem. Soc.* **1985**, *107*, 1431. (b) Baldo, M. A.; Lamansky, S.; Burrows, P. E.; Thompson, M. E.; Forrest, S. R. *Appl. Phys. Lett.* **1999**, *75*, 4.
(13) Chassot, L.; von Zelewsky, A.; Sandrini, D.; Maestri, M.; Balzani, V. *J. Am. Chem. Soc.* **1986**, *108*, 6084.
(14) (a) Barigelletti, F.; Sandrini, D.; Maestri, M.; Balzani, V.; von Zelewsky, A.; Chassot, L.; Jolliet, P.; Maeder, U. *Inorg. Chem.* **1988**, *27*, 3644. (b) Gianini, M.; Forster, A.; Haag, P.; von Zelewsky, A.; Stoeckli-Evans, H. *Inorg. Chem.* **1996**, *35*, 4889.
(15) Okada, S.; Iwawaki, H.; Furugori, M.; Kamatani, J.; Igawa, S.; Moriyama, T.; Miura, S.; Tsuboyama, A.; Takiguchi, T.; Mizutani, H. SID 02 DIGEST 1360, 2002.
(16) Su, Y. J.; Huang, H. L.; Li, C. L.; Chien, C. H.; Tao, Y. T.; Chou, P. T.; Datta, S.; Liu, R. S. *Adv. Mater*. **2003**, *15*, 884.
(17) Yang, C. H.; Tai, C. C.; Sun, I. W. *J. Mater. Chem*. **2004**, *14*, 947.
(18) Rayabarapu, D. K.; Paulose, B. M. J. S.; Duan, J. P.; Cheng, C. H. *Adv. Mater*. **2005**, *17,* 349.

10.1021/om050638p CCC: $30.25
Publication on Web 11/05/2005

Scheme 1. Synthesis of the Iridium(III) Complexes

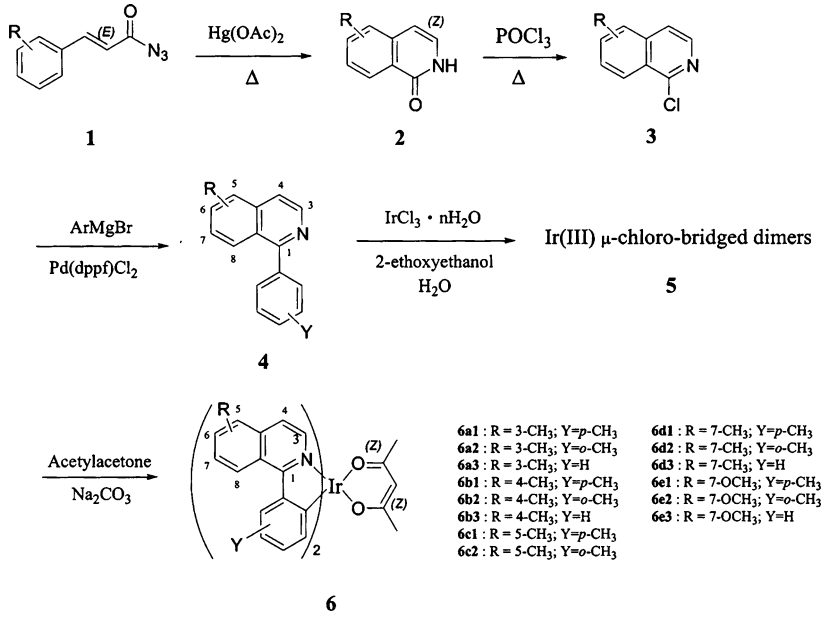

utilized for preparing a series of $(C\wedge N)_2Ir(acac)$ complexes. All synthetic procedures and manipulations involving $IrCl_3{\cdot}H_2O$ and other Ir(III) species were carried out under nitrogen. Column chromatography was carried out using 70−230 mesh silica gel. Melting points were taken on a Buchi 535 melting-point apparatus. Infrared spectra were recorded on a Nicolet Magna FT-IR spectrometer as either a thin film or solid dispersion in KBr. Nuclear magnetic resonance spectra, ^1H NMR and ^{13}C NMR, were examined in CD_2Cl_2 solution on Bruker Avance-300 (300 MHz) or AMX-400 (400 MHz) NMR spectrometers with tetramethylsilance (TMS) as the internal standard; all chemical shifts were reported in ppm from tetramethylsilane as an internal standard. Elemental analyses were performed on a Heraeus CHN-RAPID elemental analyzer and Elementar vario EL III analyzer. The EI-mass spectra were recorded on a Bruker APEX II and a VG 70-250S spectrometer. HRMS spectra were obtained using a MAT-95XL high-resolution mass spectrometer. The UV−vis spectra were measured in a 1.0×10^{-5} M CH_2Cl_2 solution on an Agilent 8453 spectrophtometer, and the photoluminescence spectra were recorded in a 1.0×10^{-5} M CH_2Cl_2 solution with a Hitachi model F-2500 fluorescence spectrophotometer.

Ligand Synthesis. General Procedure for the Preparation of 1-Phenylisoquinolines (4). A mixture of cinnamoyl azide (**1**) (30 mmol) and mercury(II) acetate ($Hg(OAc)_2$) (0.48 g, 1.5 mmol) in *o*-dichlorobenzene (120 mL) was refluxed for 1 to 30 h. After cooling to room temperature, the precipitated product was collected by filtration, washed with hexane (2×25 mL), and dried to yield a pale yellow solid (**2**). A mixture of **2** (30 mmol) and $POCl_3$ (35 mL, 0.38 mol) was refluxed for 3 h. After cooling to 60 °C, the excess amount of $POCl_3$ was distilled under a vacuum. The mixture was treated with ice water and basified with aqueous 4 N NaOH, and the resulting mixture was extracted with CH_2Cl_2 (3×100 mL). The combined extracts were dried over magnesium sulfate, then the solvent was evaporated out. The residue was chromatographed on a silica gel column, eluting with *n*-hexane−EtOAc (20:1). The solid obtained was recrystallized from *n*-hexane to give 1-chloroquinoline (**3**) as white needles. A dried two-necked flask was charged under nitrogen with 1-chloroisoquinoline (**3**) (10 mmol), 1,1′-bis(diphenylphosphino)-ferrocene palladium(II) dichloride ($Pd(dppf)Cl_2$) (2.5 mg, 0.003 mmol), and dry THF (15 mL). A solution of phenylmagnesium chloride (2 M in THF, 6.0 mL, 12 mmol) was added via syringe at room temperature, causing an immediate color change to dark brown and then finally to violet. The resulting mixture was stirred for 3 h at 50 °C. After cooling, the solution was diluted with EtOAc and was carefully quenched with water. Standard extraction followed by column chromatography over silica gel eluting with *n*-hexane−EtOAc (10:1) yielded pure 1-phenylisoquinoline (**4**).

3-Methyl-1-*p*-tolylisoquinoline (4a1). Yield: 92%; white needles, mp 81−82 °C (*n*-hexane) (lit.[19] 81−82 °C); IR (KBr) ν_{max} 3051, 1620 cm^{-1}; ^1H NMR ($CDCl_3$) δ 2.44 (3H, s), 2.73 (3H, s), 7.32 (2H, d, $J = 7.8$ Hz), 7.41 (1H, t, $J = 8.2$ Hz), 7.45 (1H, s), 7.57 (2H, t, $J = 7.8$ Hz), 7.60 (1H, t, $J = 8.2$ Hz), 7.75 (1H, d, $J = 8.2$ Hz), 8.03 (1H, d, $J = 8.2$ Hz); ^{13}C NMR ($CDCl_3$) δ 21.3, 24.4, 117.7, 124.9, 126.0, 126.3, 127.6, 129.0, 129.8, 136.8, 137.5, 138.2, 150.8, 160.3; EIMS *m/z* (rel int) 233 (100, M^+). Anal. Calcd for $C_{17}H_{15}N$: C, 87.52; H, 6.48; N, 6.00. Found: C, 87.55; H, 6.53; N, 5.95.

3-Methyl-1-*o*-tolylisoquinoline (4a2). Yield: 97%; white needles, mp 40−41 °C (*n*-hexane); IR (KBr) ν_{max} 3058, 1622 cm^{-1}; ^1H NMR ($CDCl_3$) δ 2.06 (3H, s), 2.76 (3H, s), 7.34 (4H, m), 7.39 (1H, d, $J = 7.2$ Hz), 7.50 (1H, s), 7.57 (1H, d, $J = 8.1$ Hz), 7.63 (1H, d, $J = 7.2$ Hz), 7.77 (1H, d, $J = 8.1$ Hz); ^{13}C NMR ($CDCl_3$) δ 19.8, 24.3, 117.9, 125.5, 125.6, 126.1, 126.2, 127.4, 128.3, 129.5, 130.0, 136,4, 137.1, 138.9, 150.7, 160.8; EIMS *m/z* (rel int) 233 (100, M^+). Anal. Calcd for $C_{17}H_{15}N$: C, 87.52; H, 6.48; N, 6.00. Found: C, 87.40; H, 6.51; N, 5.94.

3-Methyl-1-phenylisoquinoline (4a3). Yield: 98%; white needles, mp 88−89 °C (*n*-hexane) (lit.[20] 89−90 °C); IR (film) ν_{max} 3056, 1621 cm^{-1}; ^1H NMR ($CDCl_3$) δ 2.75 (3H, s), 7.43 (1H, t, $J = 8.2$ Hz), 7.52 (4H, m), 7.63 (1H, t, $J = 8.2$ Hz), 7.67 (2H, d, $J = 7.0$ Hz), 7.78 (1H, d, $J = 8.2$ Hz), 8.00 (1H, d, $J = 8.2$ Hz); ^{13}C NMR ($CDCl_3$) δ 24.4, 118.0, 124.9, 126.1, 126.3, 127.5, 128.3, 128.4, 129.9, 137.6, 139.7, 150.8, 160.3; EIMS *m/z* (rel int) 219 (100, M^+). Anal. Calcd for $C_{16}H_{13}N$: C, 87.64; H, 5.98; N, 6.39. Found: C, 87.63; H, 5.97; N, 6.38.

4-Methyl-1-*p*-tolylisoquinoline (4b1). Yield: 95%; white needles, mp 93−94 °C (*n*-hexane) (lit.[19] 65−66 °C); IR (KBr) ν_{max} 3040, 1615 cm^{-1}; ^1H NMR ($CDCl_3$) δ 2.44 (3H, s), 2.63 (3H, s), 7.31 (2H, d, $J = 7.6$ Hz), 7.49 (1H, t, $J = 8.0$ Hz), 7.56 (2H, d, $J = 7.6$ Hz), 7.69 (1H, t, $J = 8.0$ Hz), 7.96 (1H, d, $J = 8.0$ Hz), 8.12 (1H, d, $J = 8.0$ Hz), 8.44 (1H, s); ^{13}C NMR ($CDCl_3$) δ 15.9, 21.2, 123.3, 126.0, 126.1, 126.5, 128.0, 128.9, 129.6, 129.8, 136.1, 136.8, 138.1, 142.0, 159.3; EIMS *m/z* (rel int) 233 (100, M^+). Anal. Calcd for $C_{17}H_{15}N$: C, 87.52; H, 6.48; N, 6.00. Found: C, 87.61; H, 6.14; N, 5.99.

4-Methyl-1-*o*-tolylisoquinoline (4b2). Yield: 78%; pale yellow syrup; IR (KBr) ν_{max} 3063, 1593 cm^{-1}; ^1H NMR ($CDCl_3$)

δ 2.06 (3H, s), 2.64 (3H, s), 7.33 (4H, m), 7.43 (1H, t, J = 8.0 Hz), 7.65 (2H, d, J = 8.0 Hz), 7.66 (1H, t, J = 8.0 Hz), 7.97 (1H, d, J = 8.0 Hz), 8.46 (1H, s); ^{13}C NMR ($CDCl_3$) δ 15.8, 19.6, 123.2, 125.4, 126.2, 126.5, 126.6, 127.7, 128.1, 129.5, 129.7, 130.0, 135.5, 136.3, 139.0, 141.9, 159.7; EIMS *m/z* (rel int) 233 (16, M^+); HRESI$^+$MS calcd for $C_{17}H_{16}N$ (MH^+) 234.1283, found 234.1282.

4-Methyl-1-phenylisoquinoline (4b3). Yield: 98%; white needles, mp 51−52 °C (*n*-hexane) (lit.[21] 75−76 °C); IR (KBr) ν_{max} 3059, 1615 cm^{-1}; ^{1}H NMR ($CDCl_3$) δ 2.64 (3H, s), 7.49 (4H, m), 7.68 (3H, m), 7.98 (1H, d, J = 8.5 Hz), 8.10 (1H, d, J = 8.5 Hz), 8.46 (1H, s); ^{13}C NMR ($CDCl_3$) δ 15.9, 123.4, 126.0, 126.3, 126.6, 127.9, 128.2, 128.3, 129.7, 129.9, 136.1, 139.7, 142.0, 159.2; EIMS *m/z* (rel int) 219 (14, M^+). Anal. Calcd for $C_{16}H_{13}N$: C, 87.64; H, 5.98; N, 6.39. Found: C, 87.78; H, 6.04; N, 6.40.

5-Methyl-1-*p*-tolylisoquinoline (4c1). Yield: 88%; white needles, mp 85−86 °C (*n*-hexane); IR (KBr) ν_{max} 3030, 1612 cm^{-1}; ^{1}H NMR ($CDCl_3$) δ 2.43 (3H, s), 2.66 (3H, s), 7.31 (2H, d, J = 7.8 Hz), 7.36 (1H, t, J = 7.6 Hz), 7.46 (1H, d, J = 7.6 Hz), 7.57 (2H, t, J = 7.8 Hz), 7.70 (1H, t, J = 5.8 Hz), 7.95 (1H, d, J = 7.6 Hz), 8.62 (1H, d, J = 5.8 Hz); ^{13}C NMR ($CDCl_3$) δ 18.9, 21.2, 11.60, 125.7, 126.3, 126.6, 128.8, 129.8, 130.1, 133.5, 136.1, 136.9, 138.1, 142.0, 161.1; EIMS *m/z* (rel int) 233 (100, M^+). Anal. Calcd for $C_{17}H_{15}N$: C, 87.52; H, 6.48; N, 6.00. Found: C, 87.52; H, 6.58; N, 5.97.

5-Methyl-1-*o*-tolylisoquinoline (4c2). Yield: 83%; white needles, mp 117−118 °C (*n*-hexane); IR (KBr) ν_{max} 3056, 1589 cm^{-1}; ^{1}H NMR ($CDCl_3$) δ 2.05 (3H, s), 2.73 (3H, s), 7.36 (5H, m), 7.50 (2H, m), 7.80 (1H, d, J = 5.9 Hz), 8.64 (1H, d, J = 5.9 Hz); ^{13}C NMR ($CDCl_3$) δ 18.9, 19.7, 116.3, 125.5, 125.6, 126.6, 127.4, 128.3, 129.5, 130.2, 130.4, 133.7, 135.8, 136.4, 139.4, 142.1, 161.8; EIMS *m/z* (rel int) 175 (100, M^+). Anal. Calcd for $C_{17}H_{15}N$: C, 87.52; H, 6.48; N, 6.00. Found: C, 87.54; H, 6.48; N, 6.01.

7-Methyl-1-*p*-tolylisoquinoline (4d1). Yield: 98%; white needles, mp 93−94 °C (*n*-hexane); IR (KBr) ν_{max} 3048, 1614 cm^{-1}; ^{1}H NMR ($CDCl_3$) δ 2.45 (6H, s), 7.33 (2H, d, J = 7.8 Hz), 7.47 (1H, d, J = 8.2 Hz), 7.54 (1H, d, J = 5.7 Hz), 7.59 (2H, d, J = 7.8 Hz), 7.73 (1H, d, J = 8.2 Hz), 7.87 (1H, s), 8.52 (1H, d, J = 5.7 Hz); ^{13}C NMR ($CDCl_3$) δ 21.3, 21.9, 119.5, 126.3, 126.7, 126.9, 129.0, 129.8, 132.1, 135.1, 136.9, 138.2, 141.5 (2 × C), 160.0; EIMS *m/z* (rel int) 233 (44, M^+). Anal. Calcd for $C_{17}H_{15}N$: C, 87.52; H, 6.48; N, 6.00. Found: C, 87.46; H, 6.48; N, 5.95.

7-Methyl-1-*o*-tolylisoquinoline (4d2). Yield: 88%; pale yellow syrup; IR (KBr) ν_{max} 3048, 1587 cm^{-1}; ^{1}H NMR ($CDCl_3$) δ 2.07 (3H, s), 2.42 (3H, s), 7.32 (5H, m), 7.50 (1H, d, J = 8.4 Hz), 7.61 (1H, d, J = 5.7 Hz), 7.77 (1H, d, J = 8.4 Hz), 8.55 (1H, d, J = 5.7 Hz); ^{13}C NMR ($CDCl_3$) δ 19.7, 21.8, 119.6, 125.5, 126.0, 126.7, 127.5, 128.2, 129.5, 130.2, 132.3, 134.6, 136.4, 137.1, 139.2, 141.4, 160.6; EIMS *m/z* (rel int) 233 (100, M^+). Anal. Calcd for $C_{17}H_{15}N$: C, 87.52; H, 6.48; N, 6.00. Found: C, 87.27; H, 6.60; N, 5.96.

7-Methyl-1-phenylisoquinoline (4d3). Yield: 98%; white needles, mp 51−52 °C (*n*-hexane) (lit.[22] 103−104 °C); IR (KBr) ν_{max} 3051, 1587 cm^{-1}; ^{1}H NMR ($CDCl_3$) δ 2.45 (3H, s), 7.51 (4H, m), 7.58 (1H, d, J = 5.7 Hz), 7.68 (2H, dd, J = 7.4, 0.9 Hz), 7.76 (1H, d, J = 8.4 Hz), 7.84 (1H, s), 8.54 (1H, d, J = 5.7 Hz); ^{13}C NMR ($CDCl_3$) δ 21.9, 119.6, 126.1, 126.7, 126.8, 128.2, 128.3, 129.8, 132.1, 135.0, 137.0, 139.7, 141.4, 159.9; EIMS *m/z* (rel int) 219 (100, M^+). Anal. Calcd for $C_{16}H_{13}N$: C, 87.64; H, 5.98 N, 6.39. Found: C, 87.71; H, 6.03; N, 6.40.

7-Methoxy-1-*p*-tolylisoquinoline (4e1). Yield: 94%; white needles, mp 97−98 °C (*n*-hexane); IR (KBr) ν_{max} 3007, 1625 cm^{-1}; ^{1}H NMR ($CDCl_3$) δ 2.46 (3H, s), 3.81 (3H, s), 7.34 (1H, d, J = 8.9 Hz), 7.34 (2H, d, J = 7.8 Hz), 7.42 (1H, s), 7.55 (1H, d, J = 5.5 Hz), 7.62 (2H, d, J = 7.8 Hz), 7.77 (1H, d, J = 8.9 Hz), 8.49 (1H, d, J = 5.5 Hz); ^{13}C NMR ($CDCl_3$) δ 21.3, 55.3, 105.2, 119.4, 122.8, 127.8, 128.5, 129.1, 129.5, 132.4, 137.0, 138.2, 140.5, 158.2, 159.2; EIMS *m/z* (rel int) 249 (61, M^+). Anal. Calcd for $C_{17}H_{15}ON$: C, 81.90; H, 6.06; N, 5.62. Found: C, 81.94; H, 6.13; N, 5.63.

7-Methoxy-1-*o*-tolylisoquinoline (4e2). Yield: 78%; pale yellow syrup; IR (KBr) ν_{max} 3047, 1625 cm^{-1}; ^{1}H NMR ($CDCl_3$) δ 2.09 (3H, s), 3.71 (3H, s), 6.89 (1H, d, J = 1.9 Hz), 7.33 (5H, m), 7.59 (1H, d, J = 5.8 Hz), 7.78 (1H, d, J = 8.9 Hz), 8.50 (1H, d, J = 5.8 Hz); ^{13}C NMR ($CDCl_3$) δ 19.7, 55.2, 104.9, 119.5, 122.9, 125.6, 128.3, 128.4, 129.3, 130.3, 131.9, 136.3, 139.1, 140.4, 158.3, 159.7; EIMS *m/z* (rel int) 249 (74, M^+). Anal. Calcd for $C_{17}H_{15}ON$: C, 81.90; H, 6.06; N, 5.62. Found: C, 81.76; H, 6.19; N, 5.64.

7-Methoxy-1-phenylisoquinoline (4e3). Yield: 92%; pale yellow syrup; IR (KBr) ν_{max} 3052, 1624 cm^{-1}; ^{1}H NMR ($CDCl_3$) δ 3.80 (3H, s), 7.36 (2H, m), 7.65 (4H, m), 7.72 (2H, dd, J = 8.0, 1.4 Hz), 7.79 (1H, d, J = 8.8 Hz), 8.51 (1H, d, J = 5.7 Hz); ^{13}C NMR ($CDCl_3$) δ 55.3, 105.2, 119.7, 122.9, 127.8, 128.4, 128.5, 128.6, 129.6, 132.5, 139.8, 140.5, 158.3, 159.1; EIMS *m/z* (rel int) 235 (100, M^+); HRESI$^+$MS calcd for $C_{16}H_{14}NO$ (MH^+) 236.1075, found 236.1073.

General Information for the Preparation of Iridium-(III) Complex 6. Scheme 1 outlines the synthetic processes of an example of the iridium(III) complexes $(C\wedge N)_2Ir(acac)$. Detailed procedures of the preparation, the ^{1}H NMR spectra, and chemical analysis data of the Ir(III) complex are given below.

Synthesis of Bis[3-methyl-1-*p*-tolylisoquinolinato-*N*,*C*$^{2'}$]-iridium(III) (acetylacetonate) (6a1). The dimer $[(C\wedge N)_2Ir(\mu\text{-}Cl_2)Ir(C\wedge N)_2]$ was synthesized according to a previous paper.[23] 3-Methyl-1-*p*-tolylisoquinoline (1.08 g, 4.63 mmol) and iridium trichloride ($IrCl_3{\cdot}nH_2O$, 1.68 mmol) were dissolved in a 1:3 mixture of water and 2-ethoxylethanol. The mixture was stirred under a nitrogen stream for 15 min, then refluxed at 100 °C for 24 h. After cooling to room temperature, the dimer precipitate in the mixture was filtered off and washed with deionized water, followed by drying at 60 °C in an oven. The dimer cake (0.50 g, 0.36 mmol) was deep red, and the yield was 43%. After cyclometalated Ir(III) μ-chloro-bridged dimers were obtained, 0.40 g (0.29 mmol) of the dimer was dispersed in 2-ethoxyethanol (7.47 mL) in a flask, followed by adding acetylacetone (0.06 g) and sodium carbonate (0.34 g), and stirred under nitrogen for 15 min. After that, the mixture was refluxed at 126 °C for 15 h and cooled to room temperature, and the crude product was filtered off and washed with deionized water followed by two portions of *n*-hexane and ether. The residue was chromatographed using ethyl acetate−benzene (4:1) as eluent to afford the deep red cake in 46% yield: ^{1}H NMR (CD_2Cl_2, 300 MHz) δ 1.42 (s, 6H), 2.12 (s, 6H), 2.61 (s, 6H), 4.92 (s, 1H), 6.57 (s, 2H), 6.84 (d, J = 8.0 Hz, 2H), 7.29 (s, 2H), 7.70 (m, 4H), 7.81 (d, J = 8.0 Hz, 2H), 8.09 (d, J = 8.0 Hz, 2H), 8.91 (d, J = 8.0 Hz, 2H); ^{13}C NMR (CD_2Cl_2, 75 MHz) δ 11.2, 14.5, 17.7, 89.7, 106.7, 112.1, 114.1, 115.8, 116.1, 117.7, 120.4, 121.1, 127.3, 127.5, 128.0, 136.2, 140.7, 143.7, 161.4, 175.4; EIMS *m/z* 756, [M^+]; HREIMS calcd for $C_{39}H_{35}IrN_2O_2$ 756.2328, found 756.2336. Anal. Calcd for $C_{39}H_{35}IrN_2O_2$: C, 61.90; H, 4.66; N, 3.70. Found: C, 61.38; H, 5.16; N, 3.05.

Synthesis of Bis[4-methyl-1-*p*-tolylisoquinolinato-*N*,*C*$^{2'}$]-iridium(III) (acetylacetonate) (6b1). Yield: 82%; red solid; ^{1}H NMR (CD_2Cl_2, 300 MHz) δ 1.78 (s, 6H), 2.02 (s, 6H), 2.67 (s, 6H), 5.27 (s, 1H), 6.17 (s, 2H), 6.75 (d, J = 8.0 Hz, 2H), 7.82 (m, 4H), 8.08 (d, J = 8.0 Hz, 4H), 8.27 (s, 2H), 9.01 (d, J = 8.0 Hz, 2H); ^{13}C NMR (CD_2Cl_2, 75 MHz) δ 6.3, 11.1, 18.6, 19.9, 20.8, 46.1, 90.6, 111.6, 113.9, 116.1, 116.5, 117.2, 117.4, 119.2, 120.5, 124.6, 126.8, 128.6, 130.1, 134.6, 141.4, 157.2, 174.8; EIMS *m/z* 756, [M^+]; HREIMS calcd for $C_{39}H_{35}IrN_2O_2$

(19) Kopczynski, T. *Pol. J. Chem.* **1994**, *68*, 73.
(20) Goszczynski, S.; Kopczynski, T. *J. Org. Chem.* **1973**, *38*, 1245.
(21) Kopczynski, T. *Pol. J. Chem.* **1985**, *59*, 375.
(22) Rodionov, V. M.; Alekseeva, E. N.; Vleduts, G. *Zh. Obshch. Khim.* **1957**, *27*, 734.
(23) Nonoyama, M. *Bull. Chem. Soc. Jpn*. **1974**, *47*, 767.

756.2328, found 756.2334. Anal. Calcd for $C_{39}H_{35}IrN_2O_2 \cdot 1/2CH_2Cl_2$: C, 59.42; H, 4.55; N, 3.51. Found: C, 59.72; H, 4.90; N, 3.67.

Synthesis of Bis[4-methyl-1-*o*-tolylisoquinolinato-*N*,*C*$^{2'}$]-iridium(III) (acetylacetonate) (6b2). Yield: 69%; dark red solid; ^{1}H NMR (CD_2Cl_2, 400 MHz) δ 1.80 (s, 6H), 2.24 (s, 6H), 2.65 (s, 6H), 5.30 (s, 1H), 5.46 (s, 2H), 6.43 (t, J = 7.3 Hz, 2H), 6.68 (d, J = 7.3 Hz, 2H), 7.56 (t, J = 7.6, 2H), 7.71 (t, J = 7.6 Hz, 2H), 8.02 (d, J = 7.6 Hz, 2H), 8.19 (s, 2H); ^{13}C NMR (CD_2Cl_2, 100 MHz) δ 6.0, 13.7, 18.5, 90.8, 112.9, 114.8, 115.8, 116.1, 117.3, 118.1, 119.9, 120.1, 120.7, 126.2, 126.8, 130.0, 159.1, 175.0; EIMS *m/z* 756, [M$^+$]; HREIMS calcd for $C_{39}H_{35}IrN_2O_2$ 756.2328, found 756.2331. Anal. Calcd for $C_{39}H_{35}IrN_2O_2 \cdot 1/4CH_2Cl_2$: C, 60.68; H, 4.57; N, 3.61. Found: C, 60.29; H, 4.74; N, 3.55.

Synthesis of Bis[4-methyl-1-phenylisoquinolinato-*N*,*C*$^{2'}$]iridium(III) (acetylacetonate) (6b3). Yield: 82%; red solid; ^{1}H NMR (CD_2Cl_2, 400 MHz) δ 1.82 (s, 6H), 2.69 (s,6H), 5.32 (s,1H), 6.34 (d, J = 8.1 Hz, 2H), 6.66 (td, J = 8.1 Hz, 1.3 Hz, 2H), 6.95 (td, J = 8.1 Hz, 1.3 Hz, 2H), 7.87(m, 4H), 8.12 (d, J = 8.5 Hz, 2H), 8.20 (d, J = 8.1 Hz, 2H), 8.32 (s, 2H), 9.08 (d, J = 8.5 Hz, 2H); ^{13}C NMR (CD_2Cl_2, 100 MHz) δ 6.3, 18.6, 90.7, 110.5, 114.0, 116.3, 117.2, 117.6, 118.4, 119.5, 120.7, 123.8, 126.8, 130.1, 137.3, 141.2, 157.2, 175.0; EIMS *m/z* 728, [M$^+$]; HREIMS calcd for $C_{37}H_{31}IrN_2O_2$ 728.2015, found 728.2020. Anal. Calcd for $C_{37}H_{31}IrN_2O_2$: C, 61.05; H, 4.10; N, 3.70. Found: C, 60.96; H, 4.45; N, 3.77.

Synthesis of Bis[5-methyl-1-*p*-tolylisoquinolinato-*N*,*C*$^{2'}$]-iridium(III) (acetylacetonate) (6c1). Yield: 94%; orange-red solid; ^{1}H NMR (CD_2Cl_2, 400 MHz) δ 1.83 (s, 6H), 2.10 (s, 6H), 2.83 (s, 6H), 5.32 (s, 1H), 6.27 (s, 2H), 6.84 (d, J = 8.2 Hz, 2H), 7.72 (m, 6H), 8.17 (d, J = 8.2 Hz, 2H), 8.50 (d, J = 6.6 Hz, 2H), 8.89 (d, J = 8.0 Hz, 2H); ^{13}C NMR (CD_2Cl_2, 100 MHz) δ 9.4, 11.17, 18.5, 19.9, 90.5, 106.1, 111.7, 115.0, 116.4, 117.3, 120.0, 121.3, 124.3, 124.6, 126.8, 129.0, 130.4, 134.4, 142.0, 159.1, 174.9; EIMS *m/z* 756, [M$^+$]; HREIMS calcd for $C_{39}H_{35}IrN_2O_2$ 756.2328, found 756.2330, Anal. Calcd for $C_{39}H_{35}IrN_2O_2 \cdot 1/2C_6H_{14}$: C, 63.13; H, 5.30; N, 3.51. Found: C, 62.73; H, 5.11; N, 3.51.

Synthesis of Bis[7-methyl-1-*p*-tolyisoquinolinato-*N*,*C*$^{2'}$]-iridium(III) (acetylacetonate) (6d1). Yield: 66%; red solid; ^{1}H NMR (CD_2Cl_2, 400 MHz) δ 1.76 (s, 6H), 2.03 (s, 6H), 2.65 (s, 6H), 5.25 (s, 1H), 6.18 (s, 2H), 6.77 (d, J = 8.1 Hz, 2H), 7.46 (d, J = 6.4 Hz, 2H), 7.60 (d, J = 8.2 Hz, 2H), 7.88 (d, J = 8.2 Hz, 2H), 8.16 (d, J = 8.1 Hz, 2H), 8.36 (d, J = 6.4 Hz, 2H), 8.78 (s, 2H); ^{13}C NMR (CD_2Cl_2, 100 MHz) δ 11.2, 12.2, 18.5, 19.9, 90.5, 109.5, 111.6, 115.7, 116.6, 117.2, 119.5, 122.9, 124.5, 125.6, 128.0, 129.0, 130.0, 134.5, 141.9, 158.0, 174.9; EIMS *m/z* 756, [M$^+$]; HREIMS calcd for $C_{39}H_{35}IrN_2O_2$ 756.2328, found 756.2328. Anal. Calcd for $C_{39}H_{35}IrN_2O_2$: C, 61.90; H, 4.67; N, 3.70. Found: C, 62.37; H, 5.07; N, 3.54.

Synthesis of Bis[7-methyl-1-phenylisoquinolinato-*N*,*C*$^{2'}$]iridium(III) (acetylacetonate) (6d3). Yield: 83%; red solid; ^{1}H NMR (CD_2Cl_2, 400 MHz) δ 1.79 (s, 6H), 2.67 (s, 6H), 5.30 (s,1H), 6.33 (d, J = 7.6 Hz, 2H), 6.67 (t, J = 7.6 Hz, 2H), 6.95 (td, J = 7.6 Hz, 1.3 Hz, 2H), 7.51 (d, J = 6.3 Hz, 2H), 7.62 (d, J = 8.3 Hz, 2H), 7.90 (d, J = 8.3 Hz, 2H), 8.26 (d, J = 7.6 Hz, 2H), 8.40 (d, J = 6.3 Hz, 2H), 8.78 (s, 2H); ^{13}C NMR (CD_2Cl_2, 100 MHz) δ 12.2, 18.5, 90.6, 110.2, 110.5, 115.7, 116.8, 117.3, 118.7, 120.0, 123.1, 123.7, 125.7, 128.3, 130.0, 137.2, 141.6, 158.1, 175.0; EIMS *m/z* 728, [M$^+$]; HREIMS calcd for $C_{37}H_{31}IrN_2O_2$ 728.2015, found 728.2020. Anal. Calcd for $C_{37}H_{31}IrN_2O_2$: C, 58.50; H, 4.10; N, 3.70. Found: C, 58.97; H, 4.61; N, 4.26.

Synthesis of Bis[7-methoxy-1-*p*-tolyisoquinolinato-*N*,*C*$^{2'}$]iridium(III) (acetylacetonate) (6e1). Yield: 35%; red solid; ^{1}H NMR (CD_2Cl_2, 300 MHz) δ 1.68 (s, 6H), 1.95 (s, 6H), 3.94 (s, 6H), 5.24 (s, 1H), 6.09 (s, 2H), 6.70 (d, J = 7.9 Hz, 2H), 7.37 (m, 4H), 7.81 (d, J = 9.0 Hz, 2H), 8.05 (d, J = 7.9 Hz, 2H), 8.25 (m, 4H); ^{13}C NMR (CD_2Cl_2, 75 MHz) δ 11.1, 18.5, 45.8, 90.5, 95.5, 109.6, 111.7, 113.1, 117.5, 118.7, 118.9, 122.8, 124.6, 128.8, 129.0, 134.6, 141.6, 149.2, 157.0, 174.9; EIMS *m/z* 788, [M$^+$]; HREIMS calcd for $C_{39}H_{35}IrN_2O_4$ 788.2226, found 788.2228. Anal. Calcd for $C_{39}H_{35}IrN_2O_2$: C, 59.50; H, 4.50; N, 3.56. Found: C, 59.48; H, 4.65; N, 3.46.

Synthesis of Bis[7-methoxy-1-phenylisoquinolinato-*N*,*C*$^{2'}$]iridium(III) (acetylacetonate) (6e3). Yield: 64%; red solid; ^{1}H NMR (CD_2Cl_2, 300 MHz) δ 1.79 (s, 6H), 4.03 (s, 6H), 5.32 (s, 1H), 6.31 (d, J = 7.4 Hz, 2H), 6.65 (t, J = 7.4 Hz, 2H), 6.94 (t, J = 7.4 Hz, 2H), 7.44 (d, J = 8.9 Hz, 2H), 7.50 (d, J = 6.0 Hz, 2H), 7.91 (d, J = 8.9 Hz, 2H), 8.23 (d, J = 7.4 Hz, 2H), 8.30 (s,2H), 8.35 (d, J = 6.0 Hz, 2H); ^{13}C NMR (CD_2Cl_2, 100 MHz) δ 18.5, 19.9, 45.8, 90.6, 95.4, 110.2, 110.6, 113.4, 117.7, 118.5, 118.8, 119.0, 123.0, 123.7, 129.0, 137.3, 141.3, 149.3, 157.0, 175.0; EIMS *m/z* 760, [M$^+$]; HREIMS calcd for $C_{37}H_{31}IrN_2O_4$ 759.8829, found 759.8842. Anal. Calcd for $C_{37}H_{31}IrN_2O_4 \cdot 1/4C_6H_{14}$: C, 59.18; H, 4.42; N, 3.59. Found: C, 59.45; H, 4.49; N, 3.55.

X-ray Structural Analysis. Single-crystal X-ray diffraction data were obtained on a Siemens Smart CCD 1000 diffractometer with graphite-monochromated Mo Kα radiation, operating at 50 kV and 35 mA at 23 °C, over a 2θ range of 3.68−50.14°. Three standard reflections were measured every 197 reflections. No significant decay was observed for all samples during the data collection. Data were processed on a Pentium III PC using the Bruker AXS SHELXTL NT software package. Neutral atom scattering factors were taken from Cromer and Waber. Crystallographic refinement parameters of complexes **6a1**, **6b3**, **6e1**, and **6e3** are summarized in Table 1, and selected bond distances and angles for these complexes are listed in Table 2.

OLEDs Fabrication and Measurement. Pre-patterned ITO glasses with an effective device of area 0.16 cm^2 were cleaned in detergent for 10 min and then washed with a large amount of doubly distilled water. After being sonicated in pure water for 5 min, these glasses were dried in an oven at 180 °C for 90 min. The organic layers were deposited thermally at a rate of 0.1 nm/s and pressure of $\sim 1 \times 10^{-6}$ Torr in a deposition system. Aluminum was deposited as cathode. Electroluminescence data were measured with a SpectraScan PR650.

3. Results and Discussion

Synthesis and Characterization. Bi-substituted phenylisoquinolines (**4**) were synthesized from 1-chloroisoquinoline (**3**) and aryl Gringnard reagent via cross-coupling reaction (as shown in Scheme 1). The starting material **1** was obtained from the corresponding cinnamic acids with oxalyl chloride followed by the addition of sodium azide. Without further purification, a series of substituted isoquinolones (**2**) could be synthesized by one-pot Curtius rearrangement and cyclization of the corresponding substituted cinnamoyl azides (**1**) using $Hg(OAc)_2$ as catalyst under refluxing *o*-dichlorobenzene. According to the literature procedures,[24] isoquinoline (**2**) reacted easily with phosphorus oxychloride and transformed into 1-chloroisoquinoline (**3**). The general procedure is described in the Experimental Section. Ligands **4b2** and **4e3** are yellow oils, and we could not get reliable elemental analysis data for these two compounds. However, the HREIMS and ^{1}H and ^{13}C NMR spectra of these compounds are given in the Supporting Information.

The iridium complexes were prepared from the bi-substituted phenyl-isoquinoline ligands and iridium trichloride hydrate to form a dimer, [C∧N$_2$Ir(μ-Cl)$_2$-IrC∧N$_2$], followed by the reaction with acetylacetone in

(24) Tucker, S. C.; Brown, J. M.; Oakes, J.; Thornthwaite, D. *Tetrahedron* **2001**, *57*, 2545.

Table 1. Crystallographic Data of 6a1, 6b3, 6e1, and 6e3

	6a1	6b3	6e1	6e3
empirical formula	$C_{39}H_{35}IrN_2O_2$	$C_{37}H_{31}IrN_2O_2$	$C_{39}H_{37}IrN_2O_5$	$C_{37}H_{31}IrN_2O_4$
fw	755.89	727.84	805.91	759.84
cryst syst	monoclinic	orthorhombic	monoclinic	monoclinic
space group	$P2_1/n$	*Pbca*	*Cc*	*C*2/*c*
a (Å)	10.5280(9)	12.4090(5)	20.9550(2)	17.1759(14)
b (Å)	15.3837(13)	17.3690(10)	15.5250(2)	17.5288(14)
c (Å)	20.2382(17)	28.4470(15)	21.8250(2)	20.9671(16)
β (deg)	104.7660(2)		101.2710(10)	106.2590(2)
volume (Å^3)	3169.5(5)	6131.2(5)	6963.3(11)	6060.2(8)
Z	4	8	8	8
density (mg/cm^3)	1.584	1.577	1.537	1.666
F(000)	1504	2880	3216	3008
cryst size (mm^3)	0.50 × 0.40 × 0.40	0.18 × 0.11 × 0.03	0.32 × 0.20 × 0.12	0.10 × 0.10 × 0.10
temp (K)	294(2)	200(2)	200(2)	294(2)
no. of reflns collected	21 019	19 804	34 951	22 579
no. of indep reflns	7592 [*R*(int) = 0.0487]	5115 [*R*(int) = 0.1044]	11 687 [*R*(int) = 0.0567]	7547 [*R*(int) = 0.0505]
no. of params	397	379	847	397
final *R* indices [$I > 2\sigma(I)$]	wR2 = 0.0826, R1 = 0.0337	wR2 = 0.1516, R1 = 0.0679	wR2 = 0.1337, R1 = 0.0492	wR2 = 0.0555, R1 = 0.0362
goodness-of-fit on F^2	1.059	1.109	1.092	0.782

[a] $R1 = \sum |F_o| - |F_c|/\sum|F_o|$, $wR2 = \{\sum[w(F_o^2 - F_c^2)^2]/\sum[w(F_o^2)^2]\}^{1/2}$ (sometimes denoted as R_w^2). [b] $GooF = \{\sum[w(F_o^2 - F_c^2)^2]/(n - p)\}^{1/2}$, where *n* is the number of reflections and *p* is the total number of refined parameters.

Table 2. Bond Lengths (Å) and Bond Angles (deg) for 6a1, 6b3, 6e1, and 6e3

	Complex **6a1**		
Ir(1)−C(1)	1.972(4)	Ir(1)−C(18)	1.974(4)
Ir(1)−N(1)	2.076(3)	Ir(1)−N(2)	2.080(3)
Ir(1)−O(1)	2.161(3)	Ir(1)−O(2)	2.180(3)
N(1)−C(7)	1.350(5)	N(1)−C(15)	1.383(5)
N(2)−C(24)	1.351(5)	N(2)−C(32)	1.380(5)
C(1)−Ir(1)−C(18)	89.72(16)	C(1)−Ir(1)−N(1)	79.89(15)
C(18)−Ir(1)−N(1)	97.70(15)	C(1)−Ir(1)−N(2)	98.79(15)
C(18)−Ir(1)−N(2)	79.61(14)	N(1)−Ir(1)−N(2)	177.04(12)
	Complex **6b3**		
Ir(1)−C(16)	1.978(13)	Ir(1)−C(17)	1.981(13)
Ir(1)−N(1)	2.038(11)	Ir(1)−N(2)	1.993(11)
Ir(1)−O(1)	2.163(8)	Ir(1)−O(2)	2.159(9)
N(1)−C(1)	1.356(16)	N(1)−C(10)	1.344(17)
N(2)−C(23)	1.387(17)	N(2)−C(32)	1.359(17)
C(16)−Ir(1)−C(17)	91.1(5)	C(16)−Ir(1)−N(2)	96.8(5)
C(17)−Ir(1)−N(2)	80.8(5)	C(16)−Ir(1)−N(1)	80.7(5)
C(17)−Ir(1)−N(1)	99.3(5)	N(2)−Ir(1)−N(1)	177.4(5)
	Complex **6e1**		
Ir(1)−C(17)	1.983(13)	Ir(1)−C(18)	1.986(14)
Ir(1)−N(1)	2.024(11)	Ir(1)−N(2)	2.046(11)
Ir(1)−O(4)	2.149(10)	Ir(1)−O(3)	2.170(9)
N(1)−C(1)	1.367(17)	N(1)−C(10)	1.364(17)
N(2)−C(25)	1.356(17)	N(2)−C(34)	1.358(19)
C(17)−Ir(1)−C(18)	91.6(5)	C(17)−Ir(1)−N(1)	80.1(5)
C(18)−Ir(1)−N(1)	95.6(5)	C(17)−Ir(1)−N(2)	100.6(5)
C(18)−Ir(1)−N(2)	80.9(5)	N(1)−Ir(1)−N(2)	176.5(5)
	Complex **6e3**		
Ir(1)−C(1)	1.988(4)	Ir(1)−C(17)	1.961(4)
Ir(1)−N(1)	2.031(3)	Ir(1)−N(2)	2.018(3)
Ir(1)−O(1)	2.147(3)	Ir(1)−O(2)	2.156(3)
N(1)−C(7)	1.356(5)	N(1)−C(15)	1.369(5)
N(2)−C(23)	1.346(5)	N(2)−C(31)	1.371(5)
C(17)−Ir(1)−C(1)	97.11(17)	C(17)−Ir(1)−N(2)	79.57(15)
C(1)−Ir(1)−N(2)	97.09(16)	C(17)−Ir(1)−N(1)	100.22(15)
C(1)−Ir(1)−N(1)	79.70(16)	N(2)−Ir(1)−N(1)	176.75(14)

the presence of sodium carbonate.[25] All procedures involving Ir(III) species were carried out under a nitrogen gas atmosphere. All these materials were characterized by elemental analysis, ^{1}H and ^{13}C NMR, and mass spectrometry, whereas **6a1**, **6b3**, **6e1**, and **6e3** were further identified using single-crystal X-ray analysis to establish their three-dimensional structures.

In the synthesis of the iridium(III) complex, we found **5a2** and **6a2** could not be obtained due to the dual steric effect (from C-3 CH_3 in the isoquinoline ring and *o*-CH_3 in the phenyl ring), which was coincident with our expectations. Interestingly, **4a3**, **4c2**, **4d2**, and **4e2** can only produce their dimers (**5a3**, **5c2**, **5d2**, and **5e2**) but cannot produce the corresponding $(C\wedge N)_2Ir$ (acac) complexes. We suspect that the reaction conditions of introducing acetylacetone were too violent for **5a3**, **5c2**, **5d2**, and **5e2**. Further efforts for obtaining **6a3**, **6c2**, **6d2**, and **6e2** are currently in progress.

The crystallographic data for the four structures reported here have been deposited in the Cambridge Database: **6a1**, CCDC #276987; **6b3**, CCDC #276988; **6e1**, CCDC #276989; **6e3**, CCDC #276990. Single-crystal structures of complexes **6a1**, **6b3**, **6e1**, and **6e3** are represented with an ORTEP diagram in Figure 1. They were all obtained from solutions of dichlomathane−*n*-hexane (1:1). Despite the similarity of the structures of these four complexes, they crystallized in different space groups. Complexes **6a1**, **6b3**, **6e1**, and **6e3** belong to the monoclinic space group $P2_1/n$, the orthorhombic space group *Pbca*, the monoclinic space group *Cc*, and the monoclinic space group *C*2/*c*, respectively. The diversity of space groups of this series of complexes suggests that the packing of these complexes is very sensitive to the different substituents of the ligands. The molecular structures of the complexes are very similar to each other. As depicted in Figure 1, these four complexes reveal a distorted octahedral geometry around iridium, consisting of two cyclometalated isoquinoline ligands and one acac ligand. Because the three ligands split the d-orbitals of the central metal-iridium unequally, the crystal structures of these complexes are distorted octahedrons and prefer the *cis*-C−C, *trans*-N−N chelate disposition. All structures were solved by direct methods. All non-hydrogen atoms were refined anisotropically. The positions for all hydrogen atoms were either calculated or located directly from difference Fourier maps, and their contributions in structural

(25) Lamansky, S.; Djurovich, P.; Murphy, D.; Abdel-Razzaq, F.; Lee, H.; Adachi, C.; Burrows, P. E.; Forrest, S. R.; Thompson, M. E. *J. Am. Chem. Soc.* **2001**, *123*, 4304.

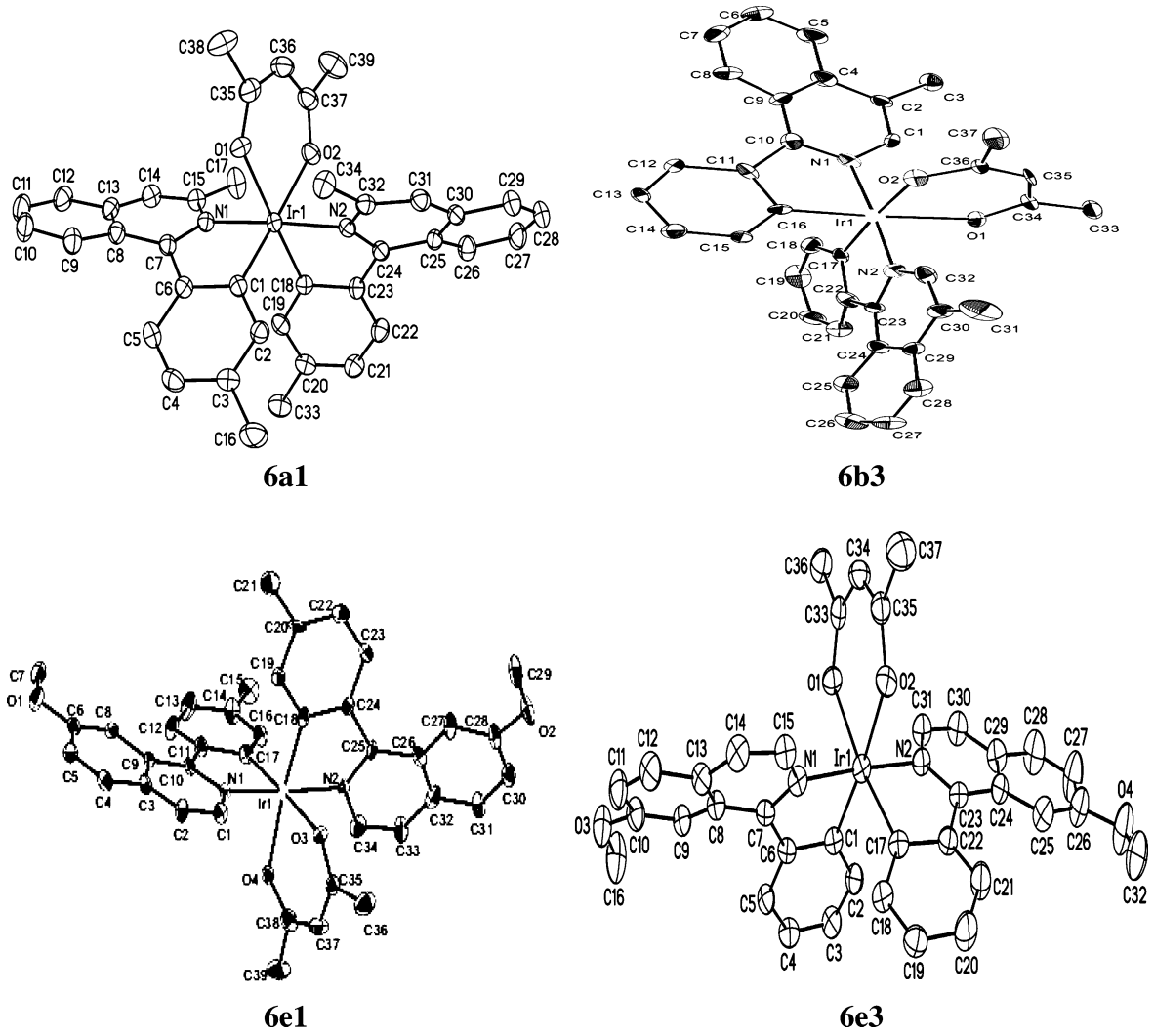

Figure 1. ORTEP diagram of **6a1**, **6b3**, **6e1**, and **6e3** with the thermal ellipsoids at the 50% probability limit.

factor calculations were included. The C−C and C−N bond lengths and angles observed in these four complexes are typical for aromatic molecules. On the other hand, the bond length of Ir−N in **6a1** ($Ir-N_{AV}$ = 2.078(3) Å), **6b3** ($Ir-N_{AV}$ = 2.015(11) Å), **6e1** ($Ir-N_{AV}$ = 2.035(11) Å), and **6e3** ($Ir-N_{AV}$ = 2.024(3) Å) is found to be longer than the Ir−C bond ($Ir-C_{AV}$ = 1.973(4) Å for **6a1**, $Ir-C_{AV}$ = 1.979(13) Å for **6b3**, $Ir-C_{AV}$ = 1.984(14) Å for **6e1**, and $Ir-C_{AV}$ = 1.974(4) Å for **6e3**). Due to the steric interactions, the phenyl groups are not coplanar with the isoquinoline group. X-ray data show that the dihedral angles between the two planes for **6a1** are much larger (29.4° and 32.6°) than those of the complexes **6b3** (18.1° and 12.2°), **6e1** (13.4° and 17.0°), and **6e3** (6.9° and 21.6°). These results suggest that the methyl group on the C-3 site of isoquinoline results in the largest hindrance among the four complexes. In addition, evidence from the Ir−N bond distances shows that the bonds in **6a1** (Ir−N(1) = 2.076(3) Å and Ir−N(2) = 2.080(3) Å) are substantially longer than those in **6b3** (Ir−N(1) = 2.038(11) Å and Ir−N(2) = 1.993(11) Å), **6e1** (Ir−N(1) = 2.024(11) Å and Ir−N(2) = 2.046(11) Å), and **6e3** (Ir−N(1) = 2.031(3) Å and Ir−N(2) = 2.018(3) Å), respectively. Furthermore, the Ir−N bond lengths also fall within the range of values reported for similar types of iridium(III) complexes.[26] A summary of the refinement details, resulting factors, bond lengths, and bond angles is given in Tables 1 and 2.

Photophysical Data. The absorption and photoluminescence spectra of iridium(III) complexes **6b2** and **6c1** in CH_2Cl_2 solutions are depicted in Figure 2. The data of all the iridium(III) complexes are summarized in Table 3. The strong absorption bands in the ultraviolet region at about 280−340 nm with distinct vibronic features are assigned to the spin-allowed intraligand $^1\pi-\pi^*$ transitions. The next lower energy in the visible region, weak absorption bands at about 440−500 nm, can be ascribed to the typical spin-allowed metal to ligand charge-transfer (^{1}MLCT) transition, while their extinction coefficients at peak wavelengths are in the range 3000−6200 M^{-1} cm^{-1}. On the other hand, the weak shoulder extending into the visible region is believed to be associated with both spin−orbit coupling enhanced $^3\pi-\pi^*$ and ^{3}MLCT (spin-forbidden metal to ligand charge-transfer) transitions.

(26) (a) Lamansky, S.; Djurovich, P.; Murphy, D. Abdel-Razzaq, F.; Kwong, R.; Tsyba, I.; Bortz, M.; Mui, B.; Bau, R.; Thompson, M. E. *Inorg. Chem*. **2001**, *40*, 1704. (b) Breu, J.; Stossel, P.; Schrader, S.; Starukhin, A.; Finkenzeller, W. J.; Yersin, H. *Chem. Mat*. **2005**, *17*, 1745.

Table 3. λ_{max} of UV−Vis and Photoluminescence Data of Iridium(III) Complexes

complex	absorbance[a] λ (nm) (log ϵ)[b]	excitation λ_{max} (nm)	emission λ_{max} (nm)[a]	$\Phi_{degassed}$[c]
6a1	287 (4.05), 361 (3.79), 472 (3.59)	472	625	0.26
6b1	302 (4.43), 346 (4.27), 472 (3.68)	472	619	0.18
6b2	289 (4.15), 348 (4.03), 485 (3.67)	485	640	0.22
6b3	297 (4.39), 341 (4.20), 472 (3.64)	472	624	0.24
6c1	289 (4.34), 348 (4.22), 472 (3.71)	472	615	0.34
6d1	289 (4.55), 348 (4.27), 472 (3.70)	472	616	0.50
6d3	289 (4.52), 347 (4.22), 472 (3.70)	472	619	0.38
6e1	280 (4.45), 376 (3.86), 472 (3.47)	472	630	0.33
6e3	280 (4.59), 375 (3.99), 471 (3.71)	471	626	0.46

[a] All data were obtained in CH_2Cl_2 solution (concentration = 10^{-5} M). [b] The unit of ϵ is M^{-1} cm^{-1}. [c] The quantum yields (Φ) in degassed CH_2Cl_2 solution were measured at 298 K and used $Ir(piq)_3$ ($\Phi = 0.6$) as a standard.

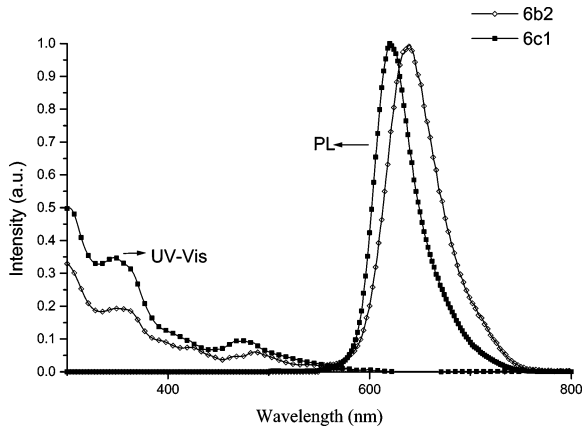

Figure 2. Normalized UV−vis and photoluminescence spectra of **6b2** and **6c1** in CH_2Cl_2 (10^{-5} M).

Highly intensive luminescence was observed for these iridium(III) complexes in CH_2Cl_2 with λ_{max} at 615−640 nm. In comparison to $(piq)_2Ir(acac)$ (bis(1-phenylisoquinolinato-*N*,$C^{2\prime}$)iridium (acetylacetonate), λ_{max} at 618 nm),[17] **6b2** shows a ~22 nm bathochromic shift in the photoluminescence peak. This red-shift effect can also be observed in the MLCT transition, as shown in Table 3. It is possible that the *o*-CH_3 of the phenyl ring brings about a steric effect in the phenyl and isoquinoline rings. Due to the steric interactions, the phenyl groups are not coplanar with the central metal and isoquinoline groups. This larger distorted angle makes the triplet energy gaps of **6b2** smaller after splitting from the ligand−iridium complex.

Redox Chemistry. Cyclic voltammetry was conducted at a Pt disk electrode (BAS Co.) in CH_2Cl_2 solutions containing 0.001 M of the iridium(III) complexes and 0.1 M tetra-*n*-butylammonium perchlorate as the supporting electrolyte. For illustration purposes, a typical voltammogram of **6c1** is shown in Figure 3 together with the voltammogram of ferrocene. The electrochemical data of these compounds are collected in Table 4. It shows that the C∧N_2Ir(III)(LX) complexes all undergo a reversible one-electron oxidation (peak potential separation ~60 mV) with no reduction process observed within the solvent cathodic potential limit. The energy level of the LUMO was evaluated from the long-wavelength absorption edge using the theory reported by Burrows et al.[27] The summarized HOMO, LUMO, and energy band gap data of all the isoquinoline derivative iridium(III) complexes shown in Table 4 are very close to each other, except the redox potentials. The $E_{1/2}$ data of iridium(III) complexes **6b1**, **6b2**, and **6e1** exhibit higher values (580−614 mV) than others (497−540 mV). This fact implies that despite the similar energy gap of these complexes, the different substitute groups at different sites on the isoquinoline ligands have a significant effect on their molecular orbital energy.

Some interesting information can be extracted from the electrochemical data. Previously, we have reported

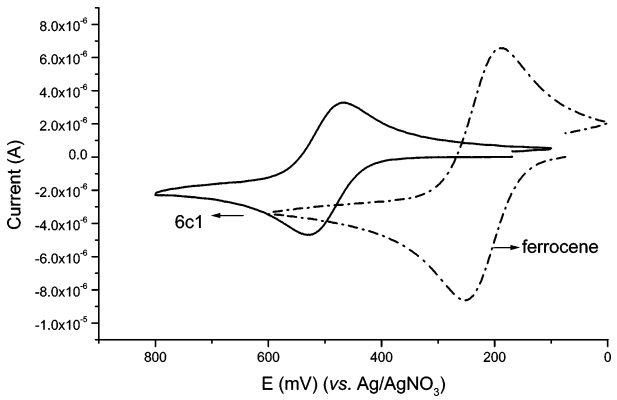

Figure 3. Cyclic voltammogram of **6c1**. CV data were measured in CH_2Cl_2 solution with Pt disk electrode, Ag/$AgNO_3$ electrode, and Pt electrode as working, reference, and counter electrode, respectively. The scan rate is 100 mV/s, using ferrocene as reference.

Table 4. Electrochemical Data, HOMO, LUMO, and Energy Gap of the Iridium(III) Complexes

complex	$E^a_{p(ox)}$ (mV)	$E^c_{p(ox)}$ (mV)	$E_{1/2(ox)}$ (mV)[a]	HOMO (eV)[c]	LUMO (eV)[d]	energy gap (eV)
6a1	527	466	497 [275][b]	−5.1	−3.1	2.0
6b1	637	572	605 [383][b]	−5.2	−3.2	2.0
6b2	609	551	580 [358][b]	−5.2	−3.1	2.1
6b3	531	470	501 [279][b]	−5.1	−3.0	2.1
6c1	531	470	501 [279][b]	−5.1	−2.9	2.2
6d1	537	477	507 [285][b]	−5.1	−2.9	2.2
6d3	570	510	540 [318][b]	−5.1	−3.1	2.0
6e1	644	583	614 [392][b]	−5.2	−3.2	2.0
6e3	573	515	544 [352][b]	−5.2	−3.1	2.1

[a] $E_{1/2(ox)} = {}^1/_2(E_p{}^a + E_p{}^c)$ (vs Ag^+/Ag). [b] $E_{1/2(ox)}$ vs ferrocene/ferrocenium. [c] Data were collected in CH_2Cl_2 solution containing 0.001 M iridium(III) complexes by cyclic voltammograms. [d] Data were collected in CH_2Cl_2 solution by UV−vis spectrophotometer.

(27) Burrows, P. E.; Shen, Z.; Bulovic, V.; McCarty, D. M.; Forrest, S. R. *J. Appl. Phys.* **1996**, *79*, 7991.

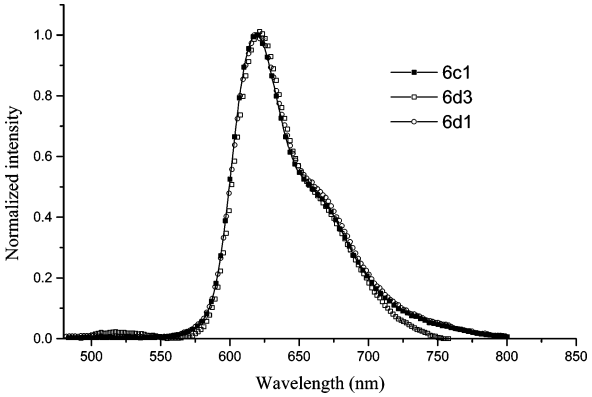

Figure 4. Electroluminescence spectra of **6c1**, **6d3**, and **6d1** at 14 V.

the nonsubstituted phenylisoquinoline iridium(III) complex, $(piq)_2Ir(acac)$.[17] The $E_{1/2(ox)}$ of $(piq)_2Ir(acac)$ is 707 mV. When an electron-donating group such as CH_3 or OCH_3 was introduced into the phenyl ring of the Ir(III) complex, the $E_{1/2(ox)}$ shifted negatively to about 631 and 695 mV, respectively. Table 4 shows that when the electron-donating group CH_3 or OCH_3 is on the isoquinoline ring (**6b3**, **6d3**, and **6e3** in Scheme 1). The $E_{1/2(ox)}$ shifts to 501, 510, and 544 mV, which indicates that the effect of introducing the electron-donating group on the isoquinoline ring is stronger than on the phenyl ring; apparently the isoquinoline-substituted Ir(III) complexes exhibited a lower HOMO energy level than the phenyl-substituted ones. In addition to **6b3**, **6d3**, and **6e3**, all the other Ir(III) complexes shown in Scheme 1 have two electron-donating groups: one is in the isoquinoline ring and another is in the phenyl ring. The data in Table 4 reveal that these bi-substituted Ir(III) complexes exhibited stronger shifting in their $E_{1/2(ox)}$ (to about 497 mV) in comparison with the monosubstituted Ir(III) complexes.

Device Properties. Using the phosphors discussed above it is possible to prepare efficient red light-emitting OLEDs. For the $(C\wedge N)_2Ir(acac)$-based devices, we have fabricated **6c1**, **6d1**, and **6d3** as dopants into the emissive layer of OLED. Devices were fabricated by high-vacuum (10^{-6} Torr) thermal evaporation on precleaned indium−tin oxide (ITO) glass substrates. The organic and metal cathode layers were grown smoothly. In our device, NPB (4,4′-bis[*N*-(1-naphthyl)-*N*-phenylamino]biphenyl) acts as the hole-transporting layer, BCP (2,9-dimethyl-4,7-diphenyl-1,10-phenanthroline) acts as the hole-blocking layer, CBP(4,4′-bis(*N*-carbazolyl)biphenyl) acts as the host, the iridium(III) complexes act as the dopant in the emitting layer, and Alq_3 (tris(8-hydroxyquinoline)aluminum(III)) acts as the electron-transport layer. The device structure and the thickness of the layers are ITO/NPB (50 nm)/CBP: 6% dopant (30 nm)/BCP (10 nm)/Alq_3 (30 nm)/LiF (1 nm)/Al). The normalized EL spectra were recorded at ∼622 nm for the devices of **6c1**, **6d1**, and **6d3**, as shown in Figure 4. Table 5 summarizes and compares the EL properties of the devices. As expected, the brightness and current density increased with increased voltage. However, the device showed a gradual decrease in luminance efficiency and power efficiency with increasing voltage. For all devices, the PL and EL spectra show similar trends, but the EL maximum is consistently red-shifted by ca. 6 nm with respect to the PL values recorded in CH_2Cl_2 solution at 298 K. Comparing the relative electroluminescent properties, the devices with **6d3** and **6d1** dopants have similar electroluminescent properties with regard to brightness, but the luminance efficiency, power efficiency, current density, and CIE are poor. We presumed that part of the injected charge carriers are recombined at the Alq_3 layers, and this affected the performance of the device. A better performance in device properties is obtained with the device using **6c1** as the dopant, showing higher brightness (9299.36 cd/m^2), better luminance efficiency (14.60 cd/A), and better power efficiency (3.28 lm/W) at higher current density (63.69 mA/cm^2). The corresponding CIE (Commission International de L'Eclairage) coordinates are $x = 0.67$, $y = 0.33$; these were close to the National Television Standards Committee recommended red for a video display. This proves that bi-substituted phenylisoquinoline iridium(III) complexes are excellent dopants for OLEDs.

Table 5. Electroluminescence Data for Iridium(III) Complexes

	6c1	6d1	6d3
brightness (cd/m^2)	62.13[a]	34.20[a]	25.56[a]
	340.48[b]	187.80[b]	163.98[b]
	1189.21[c]	697.20[c]	663.30[c]
	3311.70[d]	2154.00[d]	2077.02[d]
	9299.36[e]	6409.20[e]	6121.08[e]
luminance efficiency (cd/A)	21.96[a]	19.91[a]	11.87[a]
	18.42[b]	17.26[b]	14.07[b]
	16.52[c]	15.41[c]	13.06[c]
	15.02[d]	13.96[d]	12.30[d]
	14.60[e]	12.80[e]	11.81[e]
power efficiency (lm/W)	11.50[a]	10.42[a]	6.21[a]
	7.24[b]	6.78[b]	5.53[b]
	5.19[c]	4.84[c]	4.10[c]
	3.93[d]	3.66[d]	3.22[d]
	3.28[e]	2.82[e]	2.65[e]
current density (mA/cm^2)	0.28[a]	0.17[a]	0.22[a]
	1.85[b]	1.09[b]	1.16[b]
	7.20[c]	4.52[c]	5.08[c]
	22.05[d]	15.43[d]	16.89[d]
	63.69[e]	50.08[e]	51.83[e]
CIE	$x = 0.67$	$x = 0.66$	$x = 0.64$
	$y = 0.33$	$y = 0.33$	$y = 0.35$
EL (nm)	620	621	622

[a] For each parameter, the data in different rows correspond to those measured at different voltage: in this case, 6 V. [b] 8 V. [c] 10 V. [d] 12 V. [e] 14 V.

4. Conclusion

This work reports detailed synthesis and electrochemical and photophysical properties of nine red-emitting iridium(III) metal complexes using cyclometalated bi-substituted phenylisoqinoline ligands. Among these iridium(III) complexes, **6a1**, which has a methyl group on the site of C-3, shows larger hindrance in the X-ray single-crystal data. Upon photoexcitation, all the complexes are emissive in CH_2Cl_2. The emissions primarily originate from ^{3}MLCT and $^3\pi-\pi^*$ mixing. Complex **6b2** also shows a purer red emission at 640 nm. In the redox chemistry, we observed that the isoquinoline-substituted iridium(III) complexes exhibit less positive oxidation potential than isoquinoline-substituted iridium(III) complexes. Furthermore, we have fabricated the OLED device containing phosphorescent dopants of **6c1**, **6d1**, and **6d3**. The capabilities of the iridium(III)

complexes base triplet emitters as OLED dopants have been demonstrated.

Acknowledgment. This work was supported by the National Science Council of the Republic of China, Taiwan.

Supporting Information Available: X-ray crystallographic data, including cif files for complexes **6a1**, **6b3**, **6e1**, and **6e3**, are available free of charge via the Internet at http://pubs.acs.org.

OM050638P